JOURNAL OF CATALYSIS 108, 356–363 (1987)

Mechanism of Graphite Hydrogenation Catalyzed by Nickel

PETER J. GOETHEL AND RALPH T. YANG

Department of Chemical Engineering, State University of New York at Buffalo, Buffalo, New York 14260

Received February 17, 1987; revised June 22, 1987

Monolayer channeling of Ni particles (less than 2000 Å diameter) on the basal plane of graphite was studied for the catalyzed C/H_2 reaction (producing methane). The preferred wetting of Ni on the $\{10\bar{1}l\}$ zigzag edge of graphite determines the channel orientation and is also the driving force for channeling. The reaction follows these sequential steps: dissolution of carbon at monolayer step/Ni interface, diffusion of carbon in Ni, reaction of carbon with chemisorbed hydrogen at the Ni/gas interface. The last step (the surface reaction) is the rate-limiting step. The close similarity between the turnover rates of the surface reaction for monolayer channeling, deep-layer channeling, bulk reaction (using mixed Ni/C), and methanation (from $CO + H_2$) suggests that the surface reaction is the common rate-limiting step. Moreover, Ni is approximately two orders of magnitude more active than Pt for all modes of action except for methanation, where CH_4 is not the only product from Pt.

INTRODUCTION

The catalytic hydrogenation of carbon is an important reaction to study not only for the formation of hydrocarbons from coal but also for the understanding of metal catalyst–carbon interactions, which are important in methanation and Fischer–Tropsch reactions. The reaction of carbon monoxide and hydrogen to form methane and higher hydrocarbons is performed catalytically with Group VIII metals. The mechanisms that have been proposed more recently involve the formation and reaction of surface carbon; thus a better understanding of this surface carbon and its reactions is needed.

The reactions of the surface carbon have been studied with several different types of experiments. From the results a variety of mechanistic possibilities have been proposed. There are three major experimental techniques for studying surface carbon gasification. Bulk reaction rate measurements have been made by TGA or evolved gas analysis. The second is microscope observation and the third involves surface-science studies of the surface carbon and its gasification.

The predominant product of the carbon–hydrogen reaction at temperatures below about 1800 K is methane (*1*). Studies of the carbon–hydrogen reaction catalyzed by Group VIII metals (*2, 3*), and in particular by nickel (*4–7*) have been reported. The studies by Keep *et al.* (*4*) and by Baker *et al.* (*5, 6*) were *in situ* controlled-atmosphere TEM studies at 1 torr hydrogen pressure. The channels observed in the controlled-atmosphere TEM studies are many layers deep and thus are visible because of thickness contrast. These channel depths cannot be accurately determined. However, with monolayer (3.35 Å deep) etch pits and channels, which can be made visible only with the aid of gold decoration, the depth is known exactly, allowing accurate calculation of rates. The gold decoration TEM technique, first applied by Hennig (*7*) to the study of gas–graphite reactions, has helped significantly in our understanding of the uncatalyzed gas–carbon reactions (see reviews in (*8–10*)). The gold decoration technique was used in this investigation to study the mechanism of the nickel-catalyzed monolayer channeling in the graphite–hydrogen reaction. Although monolayer channeling may not

0021-9517/87 $3.00

significantly contribute to the total gasification rates, its mechanism is the same as that for deep-layer channeling, as will become apparent below. Furthermore, the similarity between the mechanism of the C + H_2 reaction and that of the methanation reaction (from CO + H_2), both catalyzed by Ni, will be shown and discussed.

EXPERIMENTAL

The carbon used in this study was a natural single-crystal graphite from Ticonderoga, New York. This graphite was employed because of its well-defined crystalline structure and ability to be cleaved into specimens thin enough for TEM observation while maintaining a large single crystal basal plane area. The techniques used to prepare the samples for TEM observation have been explained in full by Wong (*11*).

The technique of gold decoration was used to make visible the single-layer (3.35 Å depth) steps on the basal plane of graphite. The kinetics of the monolayer channeling could thus be accurately followed. The details of this technique can be found elsewhere (*11*).

The nickel catalyst was deposited on the sample by means of vacuum evaporation. The nickel source was 99.997% pure wire from Alfa Products. Upon heating in a hydrogen atmosphere the Ni rapidly sintered into small particles at temperatures higher than ca. 600°C. Details regarding the experimental apparatus and procedure can be found in previous work (*12, 13*).

Following the reaction, the samples were decorated with gold and placed in a JEOL-100U TEM for observation. The crystal orientations of the decorated graphite edges were determined by selected-area electron diffraction (*11*). The experimental variables were reaction temperature, time, and hydrogen partial pressure. Control experiments were performed which showed that there were no gas impurity effects and that gasification rate was not a function of reaction time. The stringent gas purification procedure as well as the catalyst reduction procedure are also described in our earlier work (*12, 13*).

RESULTS AND DISCUSSION

The basal plane of graphite samples contains vacancies at densities of 1–20 μm^{-2} (*9*). When exposed to reactive gases such as O_2, CO_2, and H_2O the vacancies are expanded into monolayer etch pits which can be observed with gold decoration in a TEM (*8–11*). Exposure of the basal plane to 1 atm H_2 (rigorously purified) for 10 hr at temperatures up to 1050°C produced no etch pits, showing that uncatalyzed hydrogenation did not occur under our experimental conditions. The possibility of a hydrogen spillover mechanism on the nickel-deposited basal plane of graphite was first tested. In the Ni/C/H_2 system spillover would be the dissociative adsorption of hydrogen on nickel followed by migration of hydrogen atoms across the nickel–carbon interface to the basal plane of carbon. The diffusion of hydrogen atoms across the basal plane to reactive sites such as lattice vacancies and dislocations then follows. Experiments conducted at temperatures ranging from 400 to 850°C showed no etch pits on the basal plane of graphite. Atomic hydrogen is highly reactive to edge carbon sites, creating etch pits with a turnover frequency of 32.65 s^{-1} at 717°C (*22*). Thus is is concluded that hydrogen spillover is not operative on the graphite basal plane.

As in the Pt-catalyzed graphite hydrogenation reaction, two types of origins for the monolayer channels were observed: single vacancies in the basal plane and the edge of monolayer ledges (*12*). The same evidence was also obtained for the Ni-catalyzed reaction to show that the shallow channels were indeed monolayer deep (*12*). Deep channels at various depths were also seen but are not discussed in this work.

The crystallographic orientation of the monolayer channels produced by nickel particles in the Ni/C/H_2 system is the same as that found by many others (*2, 4–6*) in studies of deep-layer channels formed by

nickel particles. A study (*12*) of Pt particles in the monolayer-channeling mode of catalysis also shows channeling orientations identical to those caused by Ni monolayer channeling particles. The nickel particle can channel in either the $\langle 11\bar{2}0\rangle$ or $\langle 10\bar{1}0\rangle$ direction, while the faceted orientation of the particles' leading edge always remains in contact with the $\{10\bar{1}l\}$ face (i.e., wetting the zigzag face). Figure 1 illustrates nickel particles channeling in the $\langle 11\bar{2}0\rangle$ direction. The reason for the preferred orientation has been discussed in detail (*12, 13*).

Rates and Mechanism of Monolayer Channeling

The monolayer channeling rates at 800°C are summarized in Fig. 2. This plot shows the rate to be proportional to the surface area of the channeling nickel particle exposed to the gas phase. The rates were calculated from the channel lengths by assuming that

(1) Ni particles were hemispherical and
(2) all channels were initiated at time zero, i.e., when the hydrogen was introduced.

Assumption (1) was made for estimating the metal surface area, although the particles were partially faceted.

The rate data show two important results:

(1) The Ni-catalyzed reaction is zero order with respect to hydrogen partial pressure.

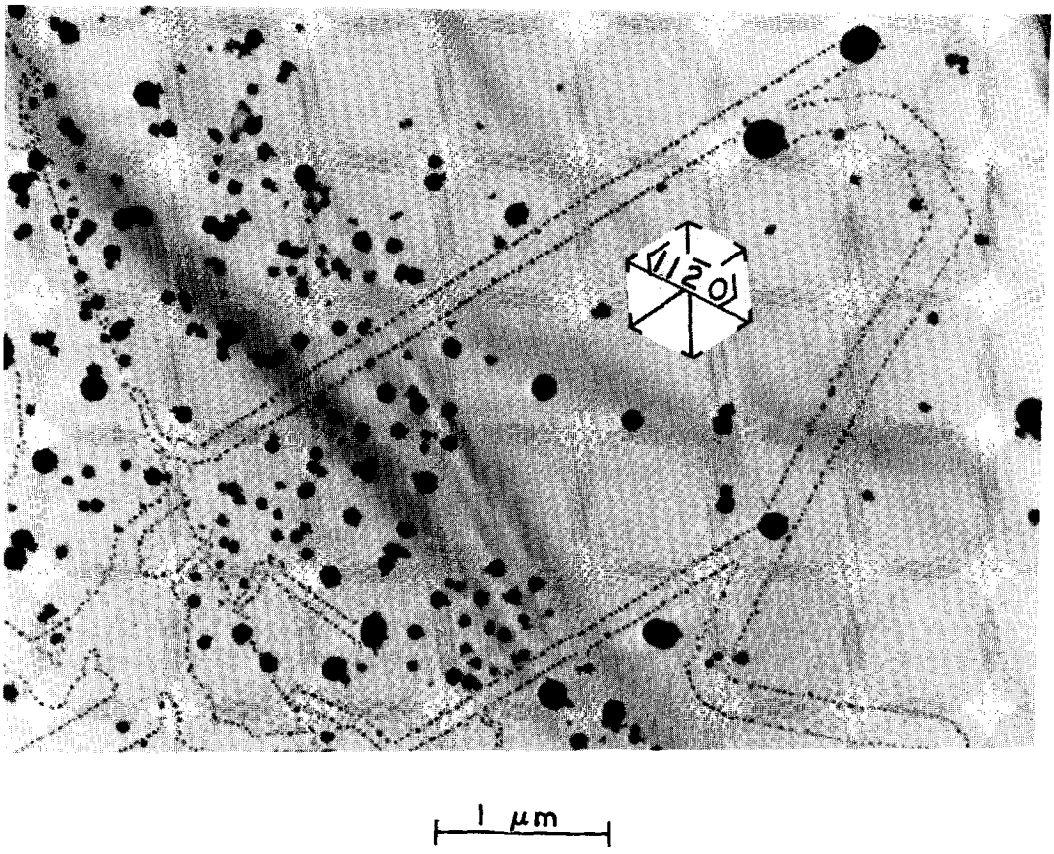

FIG. 1. Nickel particles channeling at 800°C in 1 atm hydrogen for 10 min. This illustrates nickel particles channeling in the $\langle 11\bar{2}0\rangle$ (zigzag) direction.

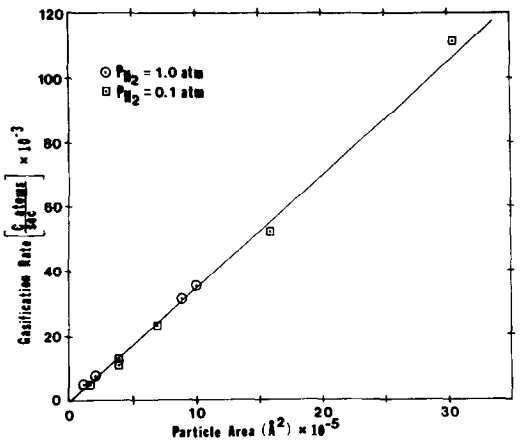

FIG. 2. For nickel particles in the monolayer channeling mode of catalysis at 800°C the gasification rate, in carbon atoms per second per channnel, is plotted versus the particle surface area exposed to the gas phase.

(2) The rate is limited by the exposed Ni surface area.

A size dependence can be seen in Fig. 3 where two particles of different diameters have channeled different lengths. The large-diameter particle channels a longer distance than the small-diameter particle. If the reaction were limited by the rate of reaction occurring at the Ni–graphite step interface then all particles would have traveled equal distances, as the graphite step is monolayer in depth. This result shows that the rate-limiting step cannot be the breaking of carbon–carbon bonds. The result also illustrates that the reaction is not diffusion controlled by products or reactants diffusing through the nickel, because diffusion control would have resulted in faster channeling for smaller-diameter particles.

The results of the rate being dependent on exposed Ni surface was previously reported by Keep *et al.* (*4*) for the Ni/C/H_2 system in an *in situ* TEM deep layer channeling study. The same dependence was also found by Baker *et al.* for Ni (*5, 6*), also in an *in situ* TEM deep-layer channeling study. The hydrogen pressure dependence was not measured in these *in situ* studies.

The result of rate dependence on exposed nickel surface area implies that the rate-limiting step is the reaction on the Ni surface. Two possible mechanisms exist. The first is the dissociative chemisorption of H_2 on nickel being rate limiting. This mechanism contradicts the observed zero-order hydrogen pressure dependence. Further evidence against the hydrogen spillover mechanism can be obtained in a calculation of the methane production rate based on the rate of chemisorption of hydrogen on Ni, assuming four chemisorbed H are needed for each CH_4 molecule. A sticking coefficient of 0.1 is assumed for an order-of-magnitude approximation (*14–17*). Using this sticking coefficient and assuming the rate to be limited by the rate of H_2 adsorption results in a CH_4 production rate of 3×10^{22} molecules/(s $\times$ cm^2 Ni) for the Ni-catalyzed carbon–hydrogen reaction at 800°C. This value is eight orders of magnitude higher than the experimental value of 3.6×10^{14} molecules/(s $\times$ cm^2 Ni). The only remaining plausible mechanism for the Ni monolayer channeling is illustated in Fig. 4. Carbon dissolves in Ni and diffuses through the Ni particle to the exposed Ni surface, where the methanation reaction takes place. An Eley–Rideal mechanism for the reaction between surface carbon and gas-phase H_2 is not important, judging from the zero-order hydrogen dependence. The rate-limiting step is thus the reaction between surface carbon and chemisorbed hydrogen on the Ni surface.

Comparison of Rates of Methanation with Monolayer, Deep-Layer Channeling and Bulk Reaction

The monolayer channeling mechanism can be directly related to the Ni-catalyzed methanation reaction (from CO and H_2) in which a carbidic carbon intermediate is involved in the reaction mechanism. Thus a direct comparison between the monolayer

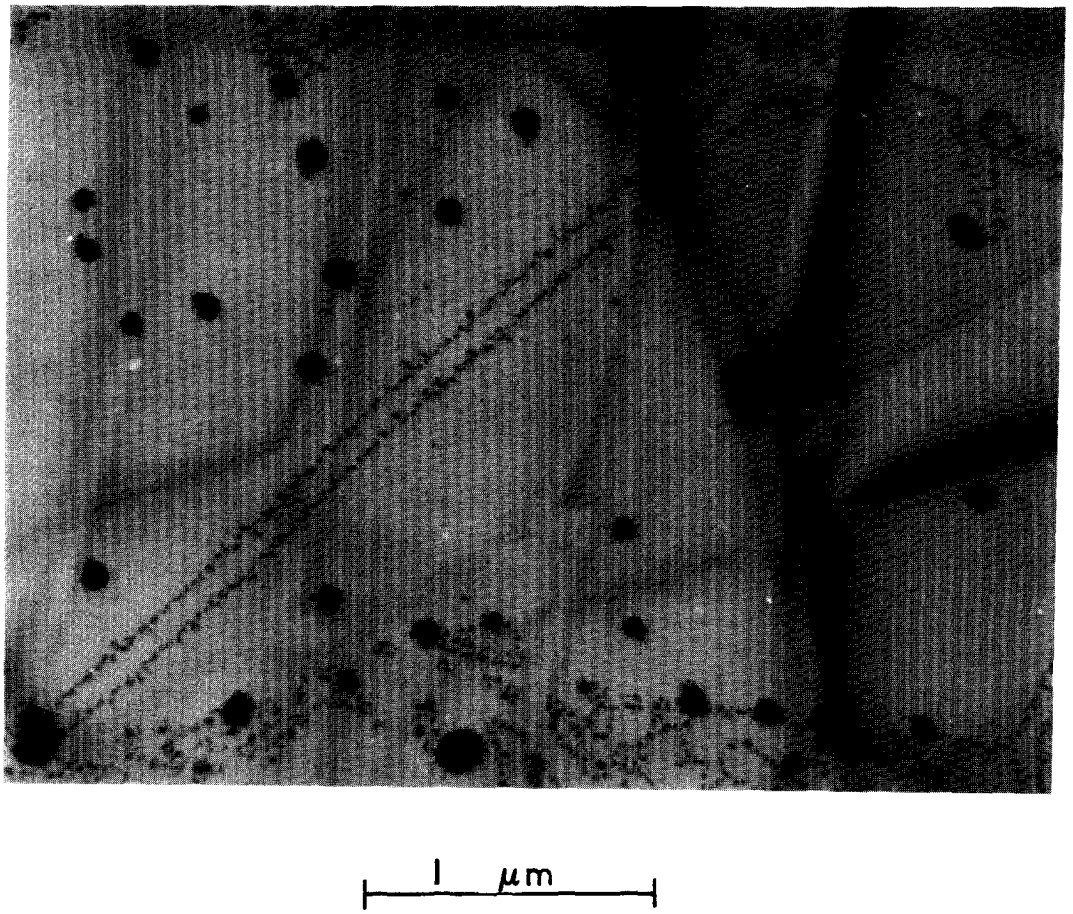

FIG. 3. Nickel particles reacted at 750°C in 1 atm hydrogen for 10 min. This illustrates larger particles channeling longer distances than smaller particles.

gasification rates obtained in this study and the methanation rates is in order.

Goodman *et al.* (*18–22*) have performed extensive studies on catalytic methanation over a single crystal Ni(100) catalyst. Their results are consistent with a mechanism in which an active surface carbon species is the dominant intermediate for CH_4 formation. Auger studies (*19*) reveal that the methane production rate (molecules/surface site/s) is a function of the surface carbon concentration. Table 1 shows their data extrapolated to a surface concentration of 0.9 and raised to 800°C.

The data by Goodman *et al.* show a linear dependence of rate on carbon coverage, X,

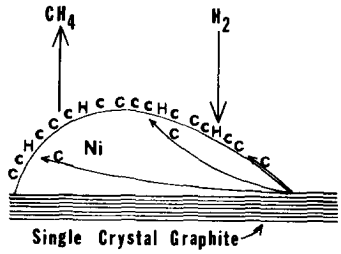

FIG. 4. Schematic representation of the mechanism for monolayer channeling in the Ni-catalyzed C–H_2 reaction. Ni wets the zigzag edge preferentially (with a smaller contact angle than on the other planes), providing the forces for movement. Surface reaction on Ni between C and H is the rate-limiting step for the particle sizes used in this study. (Sizes of Ni particles and graphite layers are not drawn to scale.)

TABLE 1

Rate of Methanation on Ni(100) of Carbon Formed from CO Disproportionation[a]

Fractional monolayer carbon coverage X	Turnover number (CH_4 molecules/Ni site/s) N_{CH_4}
0.22	4.1×10^{2}
0.43	4.1×10^{1}
0.64	4.1
0.85	4.1×10^{-1}
0.90	2.4×10^{-1}

[a] Data extrapolated to 800°C from Ref. (*19*).

from 0.15 to 0.50, which is extrapolated to $X = 0.90$. Nickel monolayer channeling at 800°C expressed on a per Ni site basis yields 2.1×10^{-1} CH_4 molecules/Ni site/s. This is an excellent agreement with their data at high carbon coverages.

A high concentration of surface carbon is plausible, as indicated by the work of Blakely *et al.* (*23–26*) on phase segregation of carbon on Ni(111). It was found in this work that a surface condensed phase (interpreted as a carbon monolayer) is precipitated on the Ni(111) face from bulk solution and has a range of stability of ~100 K. At 800°C the bulk solubility of C in Ni is 0.41 at.%. At temperatures up to 900°C a surface condensed phase of carbon on the Ni surface will be stable even though bulk solubility will have increased to 0.64 at.% and the bulk nickel concentration is only 0.41 at.% C. The reverse can then also apply for the channeling mechanism discussed in Fig. 4. Take 800°C as an example. The bulk saturated concentration of C in Ni is 0.41 at.% at 800°C and is 0.24 at.% at 700°C. Thus the carbon concentration gradient through the Ni particle can vary from the saturation value of 0.41 at.% at the Ni/graphite interface to as low as 0.24 at.% at the Ni/H_2 interface while a nearly monolayer coverage of carbon remains stable on the Ni(111) surface. No attempt was made by Blakely *et al.* (*23–26*) to study the kinetics of this condensed carbon phase formation.

The monolayer channeling rates may also be compared with the rates of (a) deep-(multi) layer channeling and (b) bulk reaction between a mixture of nickel and carbon. The rates based on per nickel surface area at 800°C are 3.5×10^{15} C atoms/s/cm^2 for deep-layer channeling (*4*) and 3.0×10^{15} C atoms/s/cm^2 for bulk reaction of Ni/carbon black/H_2 (*7*). These rates compare reasonably well with the monolayer channeling rates, further indicating a common mechanism.

Since the solubility and diffusivity of carbon in nickel at the reaction temperatures are known, it is possible to estimate if the methane formation rate can be limited by diffusion under the experimental conditions. An equilibrium solubility is assumed at the interface between graphite edge and the leading edge of nickel (see Fig. 4), i.e., 0.41 at.%. The total concentration gardient may be estimated as 0.41–0.24 at.%, or 4.7×10^{-3} g/cm^3. The diffusivity of carbon in nickel at 800°C is 1.4×10^{-8} cm^2/sec (*27*). Thus a *minimum* flux can be estimated for diffusion from the source to the farthest end of the largest particle. The diameter of the largest nickel particle was 1400 Å. Using Fick's law,

$$\text{minimum carbon flux} = \frac{D\Delta C}{L} = 2.36 \times 10^{17} \text{ C atoms/s/cm}^2$$

where D is the diffusivity, ΔC is the concentration gradient, and L is the maximum path length. This value is much greater than the measured gasification rate of 3.6×10^{14} atoms/s/cm^2. This comparison indicates that the particle must be considerably larger for carbon diffusion to be a limiting step. This comparison is, however, based on the assumption that the dissolution of carbon in nickel at the leading edge is instantaneous.

It is also interesting to compare rates for two different catalysts, Ni and Pt. For

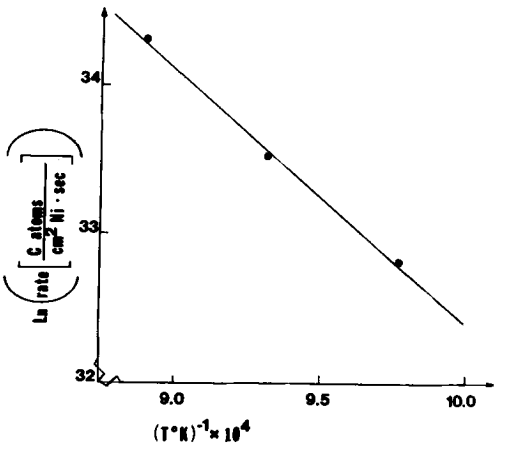

FIG. 5. Temperature dependence of the Ni-catalyzed monolayer channeling rate.

monolayer channels, the rates of Ni are two orders of magnitude higher than those of Pt. For example, the rate for Ni is 3.6×10^{14} CH_4 molecules/cm^2/s at 800°C and that for Pt is 1.5×10^{12} CH_4 molecules/cm^2/s at the same temperature (*12*). Expressed in the same rate units, Ni is also more active than Pt by about two orders of magnitude for deep-layer channeling and bulk reaction.

In deep-layer channeling Baker *et al.* (*5, 28*) found that at 1250 K Ni channeled at a rate of ~3 nm/s and Pt channeled at a rate of 0.1 nm/s for particles of similar sizes. The depths of the channels are not known and could be different, but the rates still reflect difference in catalytic activity. For bulk studies Grigor'ev *et al.* (*7*) found a Ni catalyzed gasification rate of 9.8×10^{16} C atoms/cm^2 Ni/s at 1000°C and a Pt-catalyzed gasification rate of 2.6×10^{14} C atoms/cm^2 Pt/s at 1100°C. This once again reflects the order-of-magnitude difference in catalytic activity between Ni and Pt. This is a further evidence that the same step is rate limiting for all four modes of reaction.

The temperature dependence of the monolayer channeling rate is given in Fig. 5, from which an apparent activation energy 33 ± 5 kcal/mol is obtained. Baker *et al.* (*5*) reported an activation energy of 23.6 ± 3 kcal/mol and Keep *et al.* (*4*) reported an activation energy of 53 ± 10 kcal/mol over the temperature range of 700 to 775°C. A bulk reactor study using a nickel-impregnated carbon sample was performed by Tomita *et al.* (*2*) and yielded an activation energy of 26 ± 4 kcal/mol.

Monolayer channeling was found to commence at approximately 700°C, which agrees with the observation by Keep *et al.* (*4*). Baker *et al.* (*5*), however, reported deep-layer channeling starting at 845°C. No obvious reason for these large differences in activation energy and initiation temperature can be given.

CONCLUSION

The rate of monolayer channeling for Ni-catalyzed graphite hydrogenation is considerably higher than that catalyzed by Pt, e.g., by a factor of 240 at 800°C. However, the mechanism for monolayer channeling is the same for both catalysts: breakage of C–C bonds at the interface between metal and zigzag graphite edge, dissolution of carbon in metal, diffusion of carbon to the metal/H_2 interface, followed by the surface reaction of carbon and chemisorbed hydrogen. For Ni particles with sizes below 2000 Å, the surface reaction is the rate-limiting step.

Comparison of the monolayer channeling rates with literature data on deep-layer channeling and on bulk reaction (between mixed C/Ni) indicates that the same mechanism is operative in all three modes of catalytic actions. A further comparison of the rates with methanation rates (CO + H_2) expressed as turnover frequencies suggests that they have the same rate-limiting step.

ACKNOWLEDGMENT

This work was supported by the National Science Foundation under Grant CBT-8507525.

REFERENCES

1. Holstein, W. L., and Boudart, M., *J. Catal.* **72,** 328 (1981).
2. (a) Tomita, A., and Tamai, Y., *J. Catal.* **72,** 293 (1972); (b) Tomita, A., Sato, N., and Tamai, Y., *Carbon* **12,** 143 (1974).

3. McKee, D. W., *in* "Chemistry and Physics of Carbon" (P. L. Walker, Jr., and P. A. Thrower, Eds.), Vol. 16, p. 1. Dekker, New York, 1981.
4. Keep, C. W., Terry, S., and Wells, M., *J. Catal.* **66,** 451 (1980).
5. Baker, R. T. K., and Sherwood, R. D., *J. Catal.* **70,** 198 (1981).
6. Baker, R. T. K., Sherwood, R. D., and Derouane, E. G., *J. Catal.* **75,** 382 (1982).
7. Grigor'ev, A. P., Lifshits, S. K., and Shamaev, P. P., *Kinet. Catal. (Engl. Transl.)* **18,** 948 (1977).
8. Hennig, G. R., *in* "Chemistry and Physics of Carbon" (P. L. Walker, Jr., Ed.), Vol. 2, p. 1, Dekker, New York, 1966.
9. Thomas, J. M., *Carbon* **8,** 413 (1970).
10. Yang, R. T., *in* "Chemistry and Physics of Carbon" (P. A. Thrower, Ed.), Vol. 19, p. 163. Dekker, New York, 1984.
11. Wong, C., "A Study of Carbon Gasification by Electron Microscopy," Ph.D. dissertation, State University of New York, Buffalo, New York, 1983.
12. Goethel, P. J., and Yang, R. T., *J. Catal.* **101,** 342 (1986).
13. Goethel, P. J., M.S. thesis, State University of New York, Buffalo, New York, 1986.
14. Gilbreath, W. P., and Wilson, D. E., *J. Vac. Sci. Technol.* **8,** 45 (1971).
15. Taylor, N., and Creasy, R., *in* "Adsorption–Desorption Phenomena" (F. Ricca, Ed.), p. 297. Academic Press, New York, 1972.
16. Lapajoulade, J., and Neil, K. S., *J. Chem. Phys.* **57,** 3535 (1972).
17. Lapajoulade, J., and Neil, K. S., *Surf. Sci.* **35,** 288 (1973).
18. Goodman, D. W., Kelley, R. D., Madey, T. E., and White, J. M., *J. Catal.* **64,** 479 (1980).
19. Kelley, R. D., Goodman, D. W., and Madey, T. E., *Prepr. Amer. Chem. Soc. Div. Fuel Chem.* **25**(2), 43 (1980).
20. Goodman, D. W., Kelley, R. D., Madey, T. E., and Yates, J. T., Jr., *J. Catal.* **63,** 226 (1980).
21. Goodman, D. W., and Kelley, R. D., *Surf. Sci.* **123,** L743 (1982).
22. Bischke, S. D., Goodman, D. W., and Falconer, J. L., *Surf. Sci.* **150,** 351 (1985).
23. Eizenberg, M., and Blakely, J. M., *J. Chem. Phys.* **71,** 3467 (1979).
24. Shelton, J. C., Patil, H. R., and Blakely, J. M., *Surf. Sci.* **43,** 493 (1974).
25. Eizenberg, M., and Blakely, J. M., *Surf. Sci.* **82,** 228 (1979).
26. Isett, L. C., and Blakely, J. M., *J. Vac. Sci. Technol.* **12**(1), 237 (1975).
27. Lander, J. L., Kern, H. E., and Beach, A. L., *J. Appl. Phys.* **23,** 12 (1952).
28. Baker, R. T. K., Sherwood, R. D., and Dumesic, J. A., *J. Catal.* **66,** 56 (1980).